frontiers | Frontiers in Climate

TYPE Original Research
PUBLISHED 07 March 2025
DOI 10.3389/fclim.2025.1505472

OPEN ACCESS

EDITED BY
Valentina Prigiobbe,
University of Padua, Italy

REVIEWED BY
Zhang Zhihao,
Xinjiang Institute of Ecology and Geography (CAS), China
Jiefei Mao,
Xinjiang Institute of Ecology and Geography, China
James Amonette,
Pacific Northwest National Laboratory (DOE), United States

*CORRESPONDENCE
Stefanie Helmrich
✉ stefanie.helmrich@gmail.com

RECEIVED 02 October 2024
ACCEPTED 24 February 2025
PUBLISHED 07 March 2025

CITATION
Helmrich S, Ringsby AJ and Maher K (2025) Reactive transport simulation of organic and inorganic carbon cycling following carbon dioxide sorption onto soil amendments in drylands.
Front. Clim. 7:1505472.
doi: 10.3389/fclim.2025.1505472

Reactive transport simulation of organic and inorganic carbon cycling following carbon dioxide sorption onto soil amendments in drylands

Stefanie Helmrich[1]*, Alexandra J. Ringsby[2] and Kate Maher[1]

[1]Department of Earth System Science, Stanford University, Stanford, CA, United States, [2]Department of Chemical Engineering, Stanford University, Stanford, CA, United States

Terrestrial nature-based climate solutions (NbCS) for carbon dioxide removal (CDR) are critical for mitigating climate change. However, the arid climates characteristic of drylands (aridity index <0.65) often limit the effectiveness of many NbCS. At the same time, drylands cover approximately 45% of the global land area and are threatened by soil degradation, necessitating the deployment of CDR methods for drylands that also promote soil health. Soil amendments with high CO_2 sorption capacity, such as biochar, could provide CDR potential and soil health benefits in drylands provided they do not negatively impact the large inorganic carbon pools typical of dryland soils. The dynamics of soil CO_2 are therefore critical for assessing the response of dryland systems to sorbing amendments. To assess the soil response to CO_2 sorption, we developed a 1D reactive transport model of unsaturated soils in equilibrium with dissolved inorganic carbon and calcite under varying soil respiration rates and soil amendment application conditions. The simulations highlight how alteration of soil CO_2 due to sorption by biochar affects dissolved inorganic carbon, pH, Ca^{2+}, and calcite. The transient conditions that emerge, including delayed emissions of respired CO_2, also emphasize the need to consider response times in monitoring campaigns based on CO_2 measurements. In scenarios where soil respiration is low, as is typical in drylands, sorption becomes increasingly important. Although the CDR potential of CO_2 sorption is variable and was modest relative to the overall CDR for a biochar deployment, the impacts of altered gas dynamics on soil inorganic carbon are important to consider as dryland soil amendments are developed.

KEYWORDS

carbon dioxide removal (CDR), gas sorption, soil, biochar, soil inorganic carbon, reactive transport model, CrunchFlow

1 Introduction

Nature-based climate solutions (NbCS) are considered essential to limit global warming as they represent one of the most mature carbon dioxide removal (CDR) methods, complementing the need for reductions in fossil fuel emissions (Griscom et al., 2017). NbCS rely on sustainable management of ecosystems to remove greenhouse gasses from the atmosphere while ideally addressing societal challenges associated with climate change (Chausson et al., 2020; Seddon et al., 2020). Early estimates suggest that sustainable management of forests, agricultural lands, grasslands, and wetlands could deliver over one

third of the cost-effective climate mitigation needed to limit global warming to below 2°C above pre-industrial levels until 2030 (Griscom et al., 2017).

Drylands (aridity index <0.65) (Cherlet et al., 2018) should be important targets for NbCS because they occupy over 45% of the global land area (Dregne et al., 1991; Prăvălie, 2016; Berg and McColl, 2021) and play an important role in controlling atmospheric CO_2. Soil inorganic carbon (SIC) accumulates in drylands. The SIC is present as pedogenic carbonate and forms at depth from Ca^{2+} derived from a mixture of dust inputs and *in situ* weathering and CO_2 in percolating water (Chadwick et al., 1999). If Ca^{2+} is supplied by weathering of calcium silicates, this process constitutes a carbon sink (Monger et al., 2015; Lal et al., 2021). The SIC stock in the upper 1 m of soil is estimated to be around 940 Pg C, which mostly occurs in drylands and is larger than the C pool in the biosphere (Lal, 2020; Lal et al., 2021). This SIC has turnover rates of several thousand years (Monger and Gallegos, 2000). However, climate change could increase carbon sequestration via SIC or lead to SIC being a source of carbon (Lal et al., 2000; Naorem et al., 2022). Drylands are specifically vulnerable to changes in environmental conditions (Lal et al., 2021) and it has been estimated that over 57–70% of dryland soil is degraded or prone to degradation (Dregne et al., 1991; Lal, 2004; Reynolds et al., 2007). Another study estimated that grazing, especially in arid and semi-arid regions might account for half of global SOC loss over the last 12,000 years (Sanderman et al., 2017), which would also affect SIC storage. However, soil degradation is still difficult to quantify (Verstraete et al., 2011; Prince, 2016; Wang et al., 2022).

Many NbCS have limited applicability in drylands due to water requirements. NbCS that are currently considered as highly promising for CDR are enhanced weathering (EW), reforestation, and biochar. EW requires leaching of alkalinity, which is inefficient in drylands (Calabrese et al., 2022; Zhang S. et al., 2022; Lehmann et al., 2023). Similarly, net primary productivity is limited by water availability (Ferguson and Veizer, 2007) therefore placing limits on restoration of organic carbon (C) stocks and discouraging biochar application that seeks to enhance primary productivity. Estimates of CDR for the aforementioned NbCS often consider only agricultural and forest lands (Roe et al., 2021). However, agricultural and forest lands only constitute roughly 9 and 23% of the global land area, respectively, and thus the development of effective drylands CDR strategies presents an important avenue for increasing global CDR capacity.

Another challenge for CDR in drylands is that drylands are understudied (Verstraete et al., 2011) and predictions from other climatic conditions might not be applicable. Eddy-covariance measurement, which works well to determine C uptake in forests, has been insufficient to identify drylands as source or sink of atmospheric CO_2 (Schlesinger, 2017). This has been attributed partly to pressure pumping and carbonate dissolution in combination with transport to groundwater, although these abiotic processes are thought to be insufficient to explain discrepancies between analytical methods (Schlesinger, 2017). Diurnal soil CO_2 flux behavior can be explained by diurnal changes in moisture and temperature that drive gas dissolution in soil water, however these changes do not constrain long-term changes in carbon cycling (Sagi et al., 2021). Overall monitoring only soil CO_2 efflux does not give a complete picture of C cycling in dryland soils.

For water-scarce drylands, soil amendments with high CO_2 sorption capacity could provide CDR potential and soil health benefits. Carbon-based materials such as biochar, as well as inorganic materials such as zeolite, are suitable because of their low cost, abundance, benign nature and recalcitrance (Halliday and Hatton, 2021; Garbowski et al., 2023). Biochar is highly porous with variability in pore volume, pore structure, specific surface area and functional groups related to feedstock type and production conditions (Francis et al., 2023). It also constitutes an important CDR strategy (Lehmann et al., 2021). Minerals such as zeolites are porous materials with high sorption capacity, and they are tunable and can be functionalized (Halliday and Hatton, 2021). Both materials improve soil health under a range of conditions (Mondal et al., 2021; Nepal et al., 2023).

Predicting the soil response to biochar is highly uncertain but abiotic processes involving SIC could significantly contribute to the variability of soil CO_2 fluxes after biochar amendment (Liu et al., 2016; Mosa et al., 2023). There are unfortunately relatively few field trials of biochar that completely constrain the carbon dynamics. A field study conducted in temperate and summer monsoon climate found a decrease in SIC, an increase in SOC, and depletion of water-soluble Ca^{2+} and Mg^{2+} in response to biochar additions (Lu et al., 2021), with an accompanying study pointing toward leaching of cations (Zhang et al., 2020). A biochar field study that was conducted over a range of climatic conditions found an increase in SIC with decreasing precipitation, while soil type and hydrological processes were also correlated to accumulation of SIC (Zhang et al., 2020). Studies conducted under arid or semi-arid conditions generally found an increase in SIC and reasoned that there is precipitation of calcite at deeper depths (Wang et al., 2015; Dong et al., 2019). However, studies investigating how SIC reacts to biochar addition, especially in drylands, are still scarce.

In this paper we investigate CO_2 sorption on biochar applied as a soil amendment and explore how manipulation of soil CO_2 affects C cycling in dryland soils. We will briefly review sorption data and present a reactive transport model (RTM) to elucidate the coupling between geochemical reactions and gas transport. The RTM simulates gas diffusion, dissolved inorganic carbon (DIC) and weathering of calcite under different application conditions and soil respiration rates. Although the sorption of CO_2 is relatively low (around 2%) compared to the total C in the simulated biochar, the simulated interactions between organic and inorganic C cycling can inform application and monitoring of a range of CDR methods that affect soil C dynamics. We will discuss the limitations for application and the benefits for soil health.

2 Methods

2.1 Sorption isotherm models

The model parameters for CO_2 sorption on soil amendments were based on sorption isotherms fitted to dry sorption data collected under soil-relevant gas conditions without the presence of soil (Ringsby et al., 2024) (Figure 1 and Supplementary Table S1). Dry sorption experiments with sorbent were chosen because the presence of water and soil hinders comparability between studies and makes generalization difficult. However, it should be noted that water (Davidson et al., 2013) and soil (Kwon and Pignatello, 2005) can reduce the specific sorption capacity.

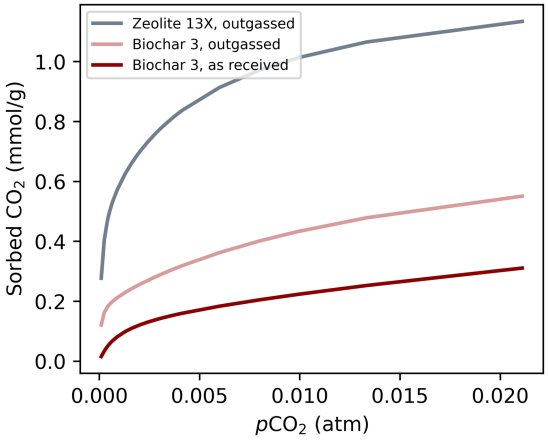

FIGURE 1
Langmuir CO_2 sorption isotherms from published data (Ringsby et al., 2024). Isotherms were fitted to data from dry sorption experiments under soil relevant conditions. Langmuir constants can be found in SI.

The sorbents were either not pre-treated before the sorption experiment ("as received") or they were outgassed at 150°C before the sorption experiment ("outgassed"). This is an important distinction because pre-treatment has been identified as a major source of uncertainty (Figini-Albisetti et al., 2010). No outgassing or an outgassing temperature that is too low will likely underestimate sorption capacity while elevated temperatures applied to temperature-sensitive materials might irreversibly alter the sorbent behavior (Figini-Albisetti et al., 2010). However, the authors also noted that the outgassing temperature must be consistent with final application. During the large-scale application process of sorbents as soil amendment, elevated temperatures are not expected. Therefore, sorption isotherms "as received," were assumed to be best in line with the intended application. The sorbent with the highest "as received" sorption capacity was Biochar 3 and was chosen for simulations, while the outgassed isotherm for Biochar 3 indicates the upper bounds likely for biochar sorbents (Ringsby et al., 2024).

A sorption isotherm model that is often used to describe experimental observations such as those above is the Langmuir model (Equations 1–3). The single site Langmuir model makes following assumptions: (1) there is a limited sorption capacity, (2) all sorption sites are equal, (3) one site sorbs one molecule of sorbent, and (4) all sites are energetically independent of the number of sorbed molecules (Limousin et al., 2007). The assumed reaction is:

$$(q_m - q) + pCO_2 \leftrightarrow q \tag{1}$$

Where q is the surface complex, q_m is the maximum sorption capacity, $q_m - q$ indicates free sites, and pCO_2 is partial pressure of CO_2. The conditional stability constant can be written as:

$$K = \frac{[q]}{[q_m - q][pCO_2]} \tag{2}$$

Where K is the Langmuir constant. The equation can be rearranged to the typical Langmuir isotherm:

$$q = \frac{q_m K\ pCO_2}{1 + K\ pCO_2} \tag{3}$$

In many cases an improved description of experimental data can be achieved with a multisite Langmuir model (Equation 4):

$$q = \sum_{i=1}^{p} \frac{q_{m,i} K_i pCO_2}{1 + K_i pCO_2} \tag{4}$$

Where K_i and $q_{m,i}$ are Langmuir constant pairs p for multiple sorption sites.

For inclusion in the reactive transport model, a multisite competitive Langmuir sorption model was adapted (Limousin et al., 2007). A reaction for a strong and a weak sorption site was implemented (Equations 5, 6):

$$> S_{strong}{}^0 + CO_2(g) \leftrightarrow > S_{strong}CO_2^0 \tag{5}$$

$$> S_{weak}{}^0 + CO_2(g) \leftrightarrow > S_{weak}CO_2^0 \tag{6}$$

Where $>S_{strong}{}^0$ refers to a strong sorption site and $> S_{weak}{}^0$ refers to a weak sorption site. The Langmuir constants K_1 and K_2 were implemented as the equilibrium constants for the two reactions. The maximum adsorption capacities $q_{m,1}$ and $q_{m,2}$ can be directly entered in the RTM. Physical properties necessary to simulate the sorbent mass were from the same published study (Supplementary Table S2). The Biochar 3 sample was obtained from Atlas Olive Oils, which produces biochar from olive tree byproducts, including pulp, pits, and branches. The chemical properties that were provided by the supplier are listed in Supplementary Table S3.

2.2 Reactive transport model

Simulations were conducted with the multi-component reactive transport code, CrunchFlow (Steefel et al., 2015). CrunchFlow allows simulation of variably saturated conditions at steady state, including gas diffusion as well as sorption of gas species. Gas diffusion was simulated via Fick's law assuming a tortuosity correction via Millington (1958). A surface complexation model (SCM) capability in CrunchFlow simulates sorption. The SCM provides flexibility to simulate sorption mechanisms or empirical sorption reactions, e.g., via the Langmuir sorption model. Equilibrium between the gas and aqueous phase is governed by Henry's law, and gas concentrations are simulated via the ideal gas law.

2.2.1 Model domain and gas transport

To simulate gas transport and C cycling in dry soil, we implemented a 1D model with 200 vertical cells representing a 2-meter soil profile. We assumed that there was no water flow, and that gas was transported only via diffusion with a free phase gas diffusion coefficient of 0.16 cm^2/s^1 (Currie, 1960; Rolston and Moldrup, 2002). A Dirichlet boundary condition was specified at the top to ensure gas diffusion between air, fixed at atmospheric CO_2 levels, and soil. A no-flow or Neumann boundary condition was set at the bottom to

simulate bedrock. Water saturation S_w was fixed to 0.4 over the whole column to simulate the presence of soil water. The value of $S_w = 0.4$ was chosen to simulate relatively dry conditions but above residual water saturation conditions (Jia et al., 2021). In the model, an increase of S_w caused an increase in pCO_2 due to lower air-filled porosity at a given CO_2 production rate. Pre-simulations showed that the same effect was achieved by varying CO_2 production. Therefore, only CO_2 production was varied to simplify interpretation of simulation outcomes.

2.2.2 Reaction network

The simulated reaction network with respect to C is shown in Figure 2. In total, eight primary and 14 secondary aqueous species were simulated including several major cations and anions that are not shown in Figure 2. Calcite was set to be in equilibrium with the aqueous phase due to its role as a pH buffer (Gaillardet et al., 1999; Wen et al., 2022; Pfeiffer et al., 2023). To simulate soil respiration a zero-order rate law assuming no inhibition or catalysis was chosen (Equation 7):

$$R = A_s \cdot k_s \tag{7}$$

Where A_s is the solid component surface area and k_s is the intrinsic rate constant. The model parameters were set such that the solid component did not decrease over the simulation time, resulting in a constant production of CO_2 over time, which simulates CO_2 emissions from the soil to the atmosphere. To reproduce observed pCO_2 depth profiles, the CO_2 production rate was simulated to be faster in the top 25 cm compared to the remainder of the profile. This idealized representation was designed to facilitate examination of the resulting dynamics in the inorganic carbon pools.

Model parameterization of aqueous, and solid phases was based on literature values (Jia et al., 2021; Wen et al., 2022) (Supplementary Tables S4, S5). The calcite mineral volume fraction was set to 3 % over the entire model based on estimates for dry climates (Pfeiffer et al., 2023). For simplicity a constant distribution of calcite over depth was considered sufficient because sorbent was only applied in the top centimeters and rain events were not simulated. A more accurate distribution of calcite over depth would be necessary for different conditions. Thermodynamic constants are from the EQ3/EQ6 database (Wolery, 1992).

2.2.3 Model approach and simulation scenarios

Prior to adding the sorbent, simulations were run to steady state to both create a baseline and exclude transient features that confuse the analysis. Depending on the initial scenario, steady- state profiles were obtained after 60–100 days. To allow all scenarios to reach steady state, the spin-up period was set to 400 days, at which point sorbent was added, and the model was run until it reached steady state again. Simulation scenarios explored variations in (1) background CO_2 production rates, (2) application rates, (3) application density, (4) application depth, and (5) increased CO_2 production after application (Supplementary Table S6).

Three simulation scenarios with low, medium, or high CO_2 production over time were developed (Supplementary Figure S2) to simulate a range of observed pCO_2 profiles (Cerling, 1984; Amundson et al., 1998; Davidson et al., 2006; Wang et al., 2013; Chirinda et al., 2014; Winnick et al., 2020). Low CO_2 production resulted in low simulated pCO_2 and might represent soil respiration rates in drylands, although it should be noted that uncertainty of CO_2 production rates is high in drylands due to data scarcity (Oertel et al., 2016; Warner

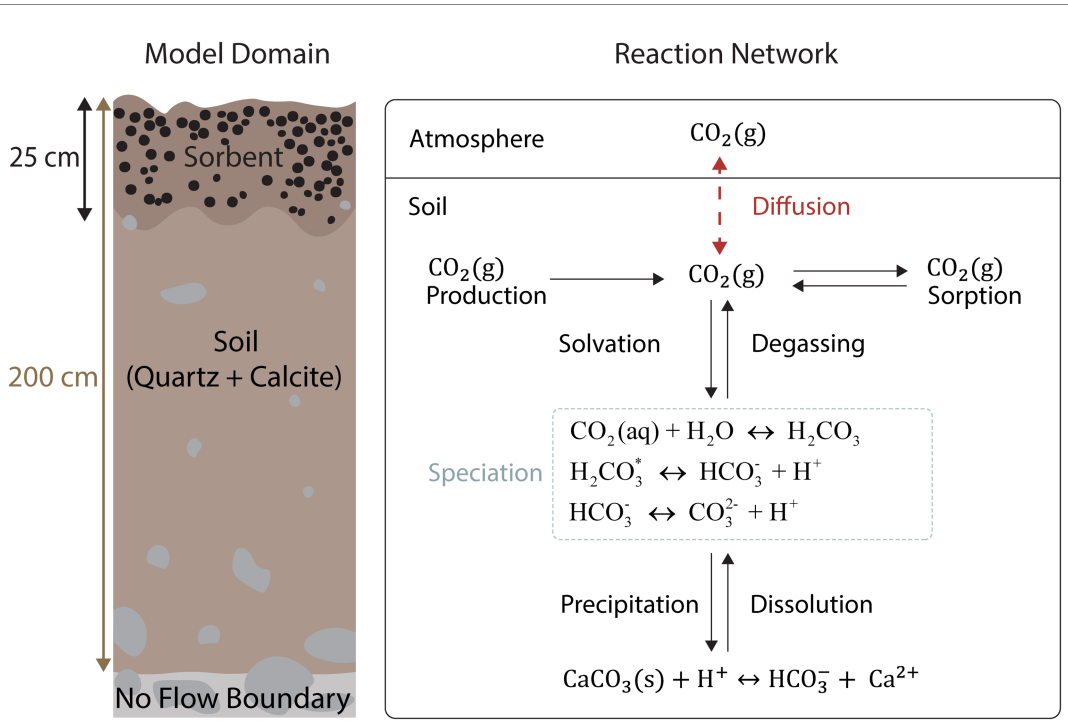

FIGURE 2
The simulated model domain (left) and the reaction network, including diffusive transport (right), are shown. When CO_2(g) dissolves in water, it becomes aqueous: CO_2(g) ↔ CO_2(aq). The convention $H_2CO_3^* = CO_2(aq) + H_2CO_3$ has been adopted.

et al., 2019). Medium and high CO_2 production rates are more typical for temperate forests and croplands (Warner et al., 2019). The medium and high rates were included because those ecosystems also occur in drylands and because soil amendments such as biochar can increase soil respiration rates (El-Naggar et al., 2019).

Application rates were varied between 2 and 20 t/acre (Lehmann and Rondon, 2006; Thengane et al., 2021). The application density, which accounts for the importance of mixing and downward physical transport of biochar (Spokas et al., 2014) was varied by changing the application depth while holding the application rate constant.

A simulated increase in CO_2 production after soil amendment application in addition to sorption (Supplementary Figure S1) was intended to replicate increased soil respiration (positive priming) that sometimes occurs after amendment of biochar, specifically in soil with initially low fertility (El-Naggar et al., 2019). Although CO_2 sorption does not directly affect soil respiration rates, most soil amendments will fundamentally alter a range of soil properties and can change soil respiration rates. For biochar, positive and negative priming have been observed in field experiments (Mosa et al., 2023). Mechanisms previously implicated in changes of CO_2 emissions after biochar application are transport effects introduced by altered pore structure (Fan et al., 2020), increased water retention, increased SOC stock, promotion of CO_2-fixing bacteria, and CO_2 sorption (El-Naggar et al., 2019; Mosa et al., 2023). Mineral soil amendments also affect soil water retention, porosity, pH, and nutrient availability (Jarosz et al., 2022; Sha et al., 2022) and could thereby alter bacterial communities (Jarosz et al., 2022; Zeng et al., 2022) and increase microbial activity (Doni et al., 2021).

To describe the relative mobility of a chemical species, a retardation factor, R_f, is often used (Freeze and Cherry, 1979). Various methods for calculation have been developed and critically reviewed (Priddle and Jackson, 1991). The relationship between R_f and porosity, bulk density, and sorption coefficients is deduced from mass balance and verified with empirical data. However, transport and scale effects can lead to variations between theoretical and field measurements (Priddle and Jackson, 1991). Methods based on breakthrough curves and times have been shown to give better results for gas–solid systems and are often applied to laboratory and field data (Priddle and Jackson, 1991; Dou et al., 2016). Here, a simulation that mimics column experiments with a constant tracer gas injection is used to simulate the effects of sorption on migration of CO_2 after sorbent deposition. A simulation scenario where only sorbent was present as solid phase was compared to a scenario where only unreactive quartz was present as solid phase. To ensure comparable diffusion, the porosity was set to 0.7 for both simulations based on biochar porosity (Gray et al., 2014). In both cases CO_2 production within the column was set to zero. However, pCO_2 was set to 30,000 ppm at the lower boundary. This ensures CO_2 diffuses through the column. When sorbent is present there will be a delay in transport. In this set up the retardation factor R_f is related to the ratio of breakthrough time of the sorbed CO_2 and the CO_2 in the unreactive quartz column (Dou et al., 2016) (Equation 8):

$$R_f = \frac{t_s}{t_u} \tag{8}$$

Where t is the time that it takes to reach half of the initial concentration in the column filled with sorbent (subscript s) and unreactive quartz (subscript u) respectively. The retardation factors were calculated from simulated concentrations at a depth of 0.75 cm. Breakthrough curves were constructed for pCO_2 at 0.5 depth.

A one-time reduction of CO_2 soil emissions was calculated as difference between simulated soil efflux without sorbent (i.e., the baseline or counterfactual) and with sorbent over the relaxation time (Equation 9):

$$\%removed = \frac{\int_{t\_i}^{t} J(t)_c\, dt - \int_{t\_i}^{t} J(t)_s\, dt}{\int_{t\_i}^{t} J(t)_c\, dt} \cdot 100 \tag{9}$$

Where J is the diffusive flux between soil and air, the subscript c indicates the counterfactual scenario, and the subscript s refers to scenarios with sorbent. Because flux J equals CO_2 production P under steady state conditions in the baseline scenario, Equation (9) can be rewritten as (Equation 10):

$$\%removed = \frac{\int_{t\_i}^{t} P_s dt - \int_{t\_i}^{t} J(t)_s\, dt}{\int_{t\_i}^{t} P_s dt} \cdot 100 \tag{10}$$

2.2.4 Model output analysis

For model verification and assessment, a time- and depth-integrated mass balance was developed (Equation 11):

$$\int_{t\_i}^{t} \frac{dCO_2}{dt} dt + \int_{t\_i}^{t} \frac{dDIC}{dt} dt + \int_{t\_i}^{t} \frac{dCalcite}{dt} dt = \int_{t\_i}^{t} P\, dt - \int_{t\_i}^{t} \frac{dU}{dt} - \int_{t\_i}^{t} J(t) dt \tag{11}$$

Where t represents time, carbon storage in the soil is calculated as the inventory of CO_2(g), DIC, and calcite, while U denotes CO_2 sorption. A detailed description of the mass balance can be found in supplemental information. The time elapsed between sorbent addition and the return of the system to steady state is the relaxation time.

3 Results

3.1 Baseline conditions under varying CO_2 production rates

Under baseline conditions with no sorbent present, simulated pCO_2 increased with depth and was higher in scenarios with higher CO_2 production (Figure 3A). The model adequately reproduced observed CO_2 trends for low, medium, and high CO_2 production where concentrations often rapidly increase to concentrations between 5,000 and 30,000 ppm over the first 50 cm (Cerling, 1984; Amundson et al., 1998; Davidson et al., 2006; Wang et al., 2013; Chirinda et al., 2014; Winnick et al., 2020). CO_2 gradients over depth (dCO_2/dz) were positive, meaning an efflux from the soil was simulated (Figure 3B). Simulated DIC increased, pH decreased and Ca^{2+} increased with depth and pCO_2 (Figures 3C–E). Depletion of the calcite mineral

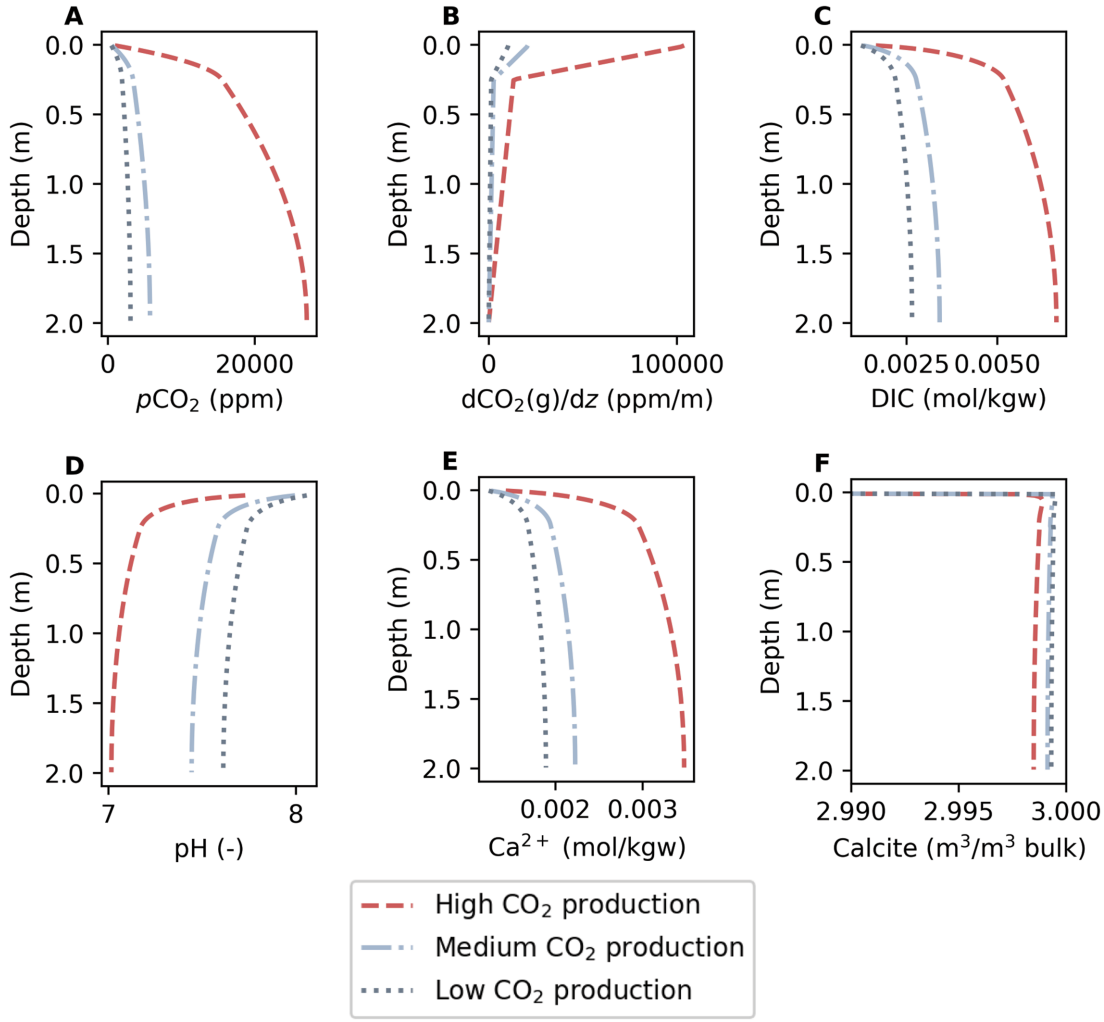

FIGURE 3
Shown are baseline conditions under constantly low, medium, and high CO_2 production. Simulated depth profiles of **(A)** pCO_2, **(B)** concentration gradient [$dCO_2(g)/dz$], **(C)** DIC, **(D)** pH, **(E)** Ca^{2+}, and **(F)** the calcite mineral volume fraction are presented.

volume fraction was higher with higher pCO_2 (Figure 3F). As noted in the methods section, the calcite distribution over depth was simplified for model interpretation and will typically vary as a function of depth depending on climate (Pfeiffer et al., 2023).

3.2 Soil CO_2 response to sorbent addition

Sorption of CO_2 affected soil pCO_2 and soil CO_2 efflux (Figure 4). The simulated sorption capacity (sorbed CO_2/g sorbent) aligned with observed data that had been used to derive sorption isotherms (Figure 4A). Sorption increases with pCO_2, which in the simulations increased with depth and CO_2 production. The scenario with the highest CO_2 production reached almost 0.015 bar within the application depth of 25 cm, under which the sorption capacity was almost three times higher than at atmospheric pCO_2. Over the simulation time, the addition of the sorbent to the soil is visible in a decline of pCO_2 (Figure 4B). At a depth of 20.5 cm, the simulated pCO_2 was initially around 2,000 ppm for a scenario with low CO_2 production. At day 400 of the simulation, sorbent was added and pCO_2 decreased to almost 0 ppm. After several days the pCO_2 rose again and then slowly returned to steady state after around 50 days. The return to steady state was faster with higher CO_2 production. Sorption behavior was transient over depth because gas diffusion and production are not instantaneous (Figure 4C). Immediately after application, sorbed CO_2 over depth followed a u-shape with high sorption at the atmosphere-soil and the shallow-deep soil interface. The shape indicates that gas from the deeper soil and the atmosphere was diffusing in (Figure 4D). The sorption temporarily reduced CO_2 efflux and even caused CO_2 influx from the atmosphere (Figure 4B). The effect on efflux lasted longer when CO_2 production was lower.

Total maximum sorption was higher with higher CO_2 production and higher total sorbent mass (Figure 5). Total sorption can be related to mean steady state pCO_2 over application depth (Supplementary Figure S3). A temporary reduction in efflux was related to CO_2 production and sorbent mass, as was expected (Figure 5B).

Transport occurred in simulations only via diffusion, which is slow compared to advection and results in a notably delayed breakthrough and broadened breakthrough curve (Figure 6)

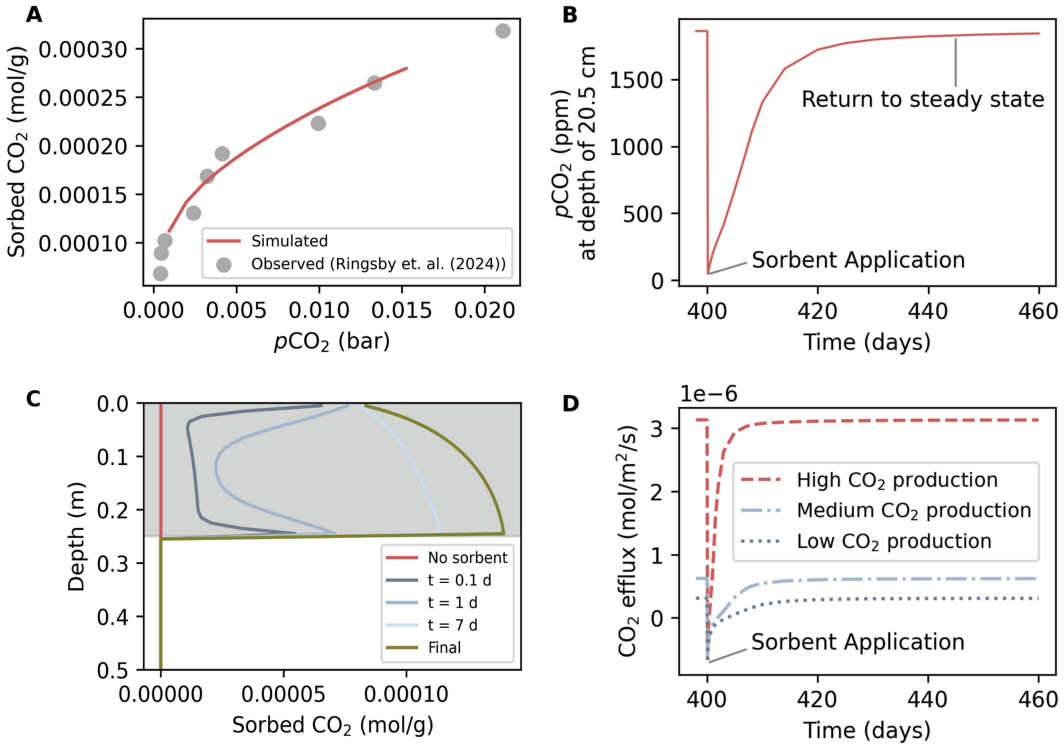

FIGURE 4
Sorbed CO_2, pCO_2 and CO_2 efflux after sorbent addition. **(A)** Sorbed CO_2 (mol/g sorbent) as a function of pCO_2 simulated under high CO_2 production (red line) and observed values that were used to fit the Langmuir isotherm (Ringsby et al., 2024) (grey dots). Sorbent was present in model over the top 25 cm. **(B)** Simulated pCO_2 over time at a depth of 0.205 m for one scenario with low CO_2 production with sorbent addition at day 400. Simulated pCO_2 was at a steady state before sorbent addition and returned to steady state after roughly 50 days. **(C)** Transient depth profiles of sorbed CO_2 over the top 0.5 m under low CO_2 production. Shown are initial baseline conditions without sorbent (red), conditions at 0.1, 1, and 7 days after sorbent application, and final sorption (green) upon which all other simulated parameters return to baseline conditions. The grey area indicates the application depth. **(D)** CO_2 efflux at soil surface with low, medium, and high CO_2 production. A drop below zero indicates influx to the soil.

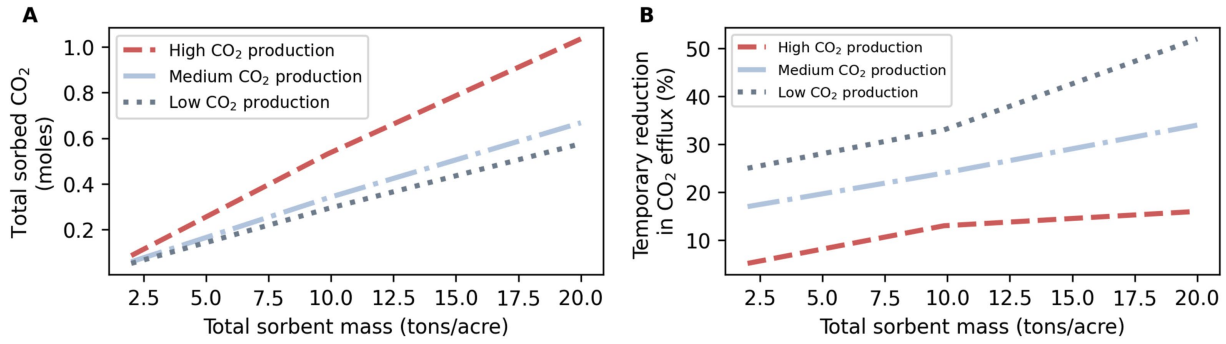

FIGURE 5
(A) Total sorbed CO_2 and **(B)** temporary reduction in CO_2 efflux, both as a function of total added sorbent mass and depending on CO_2 production.

compared with sorption studies that pump gas into columns (Kaur et al., 2019; Pal et al., 2019; Al Mesfer et al., 2020).

3.3 Response of soil geochemical parameters

Depth profiles show that changes in pCO_2 through sorption affected all simulated parameters (Figure 7). Changes are particularly visible immediately after application and where sorbent had been applied (in the top 25 cm). Immediately after sorbent application, the pCO_2 reached almost zero over the application depth. The CO_2 gradients changed from positive to negative at the atmosphere-soil interface, indicating that there was CO_2 influx to the soil instead of efflux. The CO_2 gradients strongly increased where sorbent amended soil meets the unamended soil. Over the application depth, simulated DIC was reduced by over 90%, and pH increased from 7.5 to 8. The pH was increased because sorption of CO_2 that is in equilibrium with

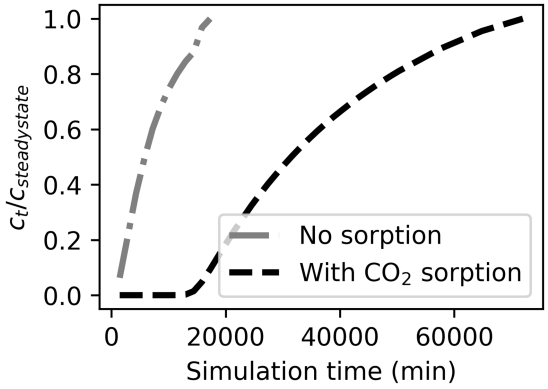

FIGURE 6
Simulated breakthrough curves for pCO_2 at 0.5 m depth when a 1 m column consists of either unreactive quartz or sorbent. Gas transport occurs only through diffusion resulting in a delay to reach steady state conditions without sorption.

the aqueous phase removes bicarbonate ions and protons from solution via:

$$CO_2(aq) + H_2O \leftrightarrow HCO_3^- + H^+ \quad (12)$$

The simulated Ca^{2+} was around 50% lower and the calcite mineral volume fraction was slightly increased due to precipitation. The precipitation was temporary, and calcite redissolved. The transient change in calcite mineral volume fraction was larger with higher total sorption. Transient conditions lasted longer when CO_2 production was lower. Transient conditions lasted for 30–50 days when only sorption and no increased CO_2 production was simulated.

Assuming an increased CO_2 production after amendment application resulted in deviation of soil geochemical parameters after 20 days (Figure 7): higher pCO_2, higher dCO_2/dz, higher DIC, lower pH, higher Ca^{2+}, and lower calcite volume fraction. This indicates that changes in CO_2 production – an empirical representation of soil respiration – have the potential to persistently change soil geochemistry.

A high retardation factor of $R_f = 37.5$ was calculated in a simplified simulation scenario with either sorbent or unreactive quartz. The delay in diffusion due to sorption is clearly visible in pCO_2 heatmaps (Figure 7). In the column with quartz, pCO_2 increases rapidly in <1 day and is then at steady state. With sorbent, there is a slow increase over 30 days, after which steady state is reached.

4 Discussion

In the following we will discuss how manipulation of soil CO_2 affects inorganic C cycling in unsaturated soils and the importance of transient conditions. We present implications for application and monitoring of CDR that affects the soil response. Although simulations were focused on C cycling, there are additional benefits and limitations for soil amendment application in drylands, which we will also discuss.

4.1 Inorganic carbon cycling in dry soils

Figure 8 shows how carbonate alkalinity and Ca^{2+} concentrations are related to carbonate dissolution via acids in addition to other processes, e.g., degassing and sorption. The 1:1 line in Figure 8 indicates carbonate dissolution through carbonic acids (Semhi et al., 2000; Perrin et al., 2008):

$$CaCO_3 + CO_2 + H_2O \leftrightarrow 2HCO_3^- + Ca^{2+} \quad (13)$$

And a possible reaction for the 2:1 line is (Zamanian et al., 2018):

$$CaCO_3 + NH_3 + H_2O + 2O_2 \rightarrow HCO_3^- + Ca^{2+} + NO_3^- + 2H_2O \quad (14)$$

Equation 14 describes calcite dissolution after N fertilizer application. Acidification leads to increased calcite dissolution rates and cations are balanced by nitrate anions, as opposed to only bicarbonate (Zamanian et al., 2018). This reaction has been identified as a CO_2 source in agricultural areas that are either limed or where carbonates naturally occur (Semhi et al., 2000; Perrin et al., 2008; Zamanian et al., 2018). Transient conditions above the 2:1 line occurred in the simulations due only to sorption and degassing—contributing to lower bicarbonate concentrations but no cations. Some calcite precipitation occurred simultaneously resulting in a slight drop in cation concentrations.

Transient conditions in drylands are often driven by wetting events, which cause a complex biogeochemical soil response (Jarvis et al., 2007) including increased soil respiration, desorption (Sánchez-García et al., 2020), and dissolution and reprecipitation of carbonate minerals (Angert et al., 2015; Gallagher and Breecker, 2020). A short-term increase in CO_2 efflux is known as "Birch effect" and is mostly attributed to increased soil respiration although immediate release of CO_2 has been associated with desorption (Kemper et al., 1985; Sánchez-García et al., 2020) which strongly depends on OM content in soils (De Jonge and Mittelmeijer-Hazeleger, 1996). Carbonate dissolution increases with elevated pCO_2, which dampens the soil CO_2 efflux after wetting events and has been associated with underestimation of soil respiration rates when carbonates are present (Angert et al., 2015; Gallagher and Breecker, 2020). A second important source of transient conditions in drylands are daily, seasonal, and annual temperature changes. Increased temperature generally leads to increased soil respiration and desorption although concomitant changes in moisture can either amplify or reduce this response (Tang et al., 2003; Shen et al., 2009; Darrouzet-Nardi et al., 2015; Sagi et al., 2021).

Transient conditions lasted for varying time scales in the simulations, which has implications for monitoring (Figure 9). Increased calcite precipitation lasted only a few hours while the soil CO_2 efflux was affected over more than 10 days. Comparison to field observations shows similar variations in time scales. The Birch effect, which occurs on dryland soils, is most pronounced for a few hours or days after a wetting event (Jarvis et al., 2007; Unger et al., 2010). Seasonal variations in wet-dry cycles will lead to prolonged variation in carbonate dissolution and precipitation (Breecker et al., 2009; Gallagher and Breecker, 2020; Domínguez-villar et al., 2022).

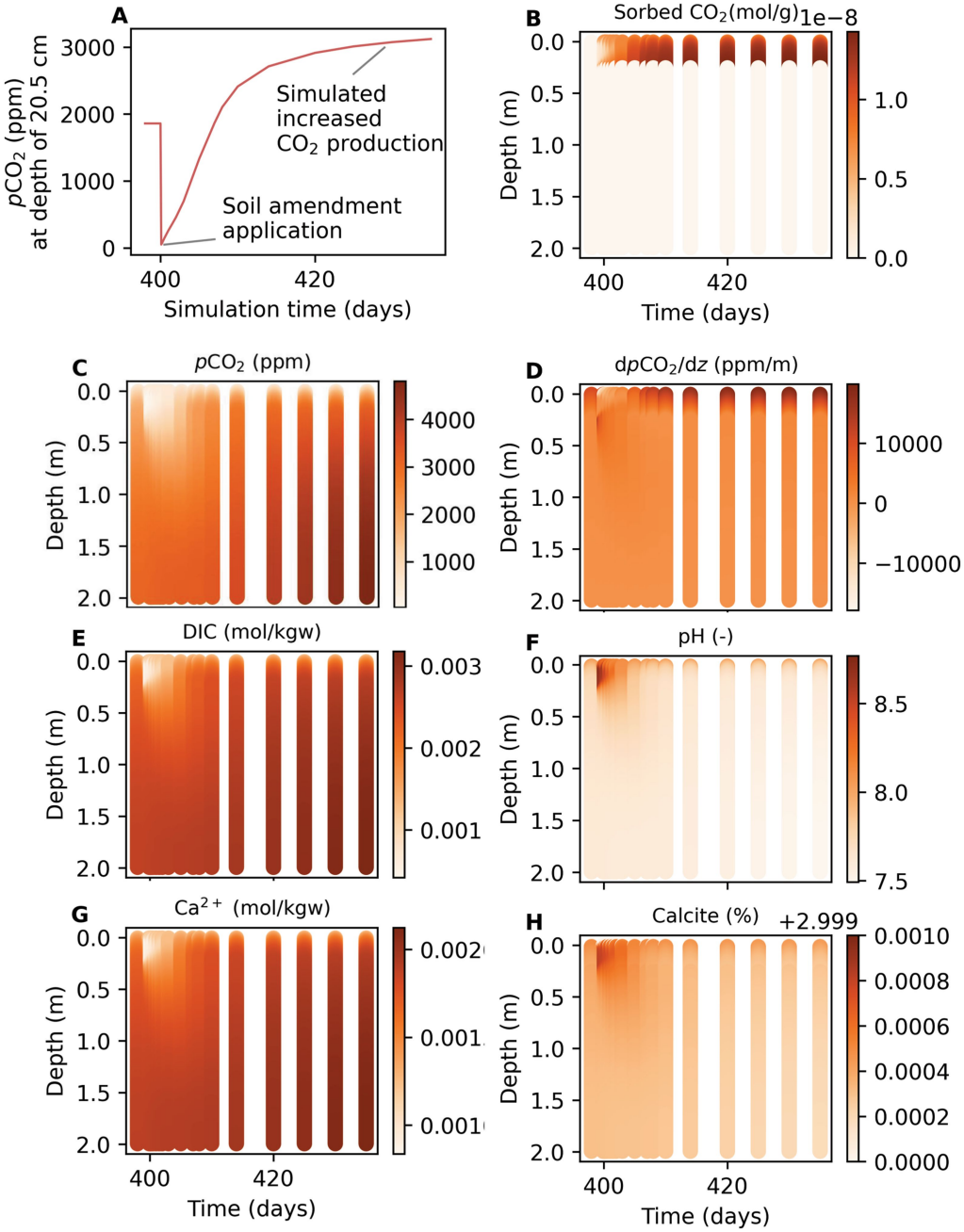

FIGURE 7
Simulated changes in soil geochemical parameters due to sorption on soil amendment and increased CO_2 production. **(A)** Simulated pCO_2 at depth 20.5 cm and over simulation time. Heatmaps over depth and simulation time for **(B)** sorbed CO_2, **(C)** pCO_2, **(D)** $dpCO_2/dz$., **(E)** DIC, **(F)** pH, **(G)** Ca^{2+}, and **(H)** calcite volume fraction. Application rate of 9.86 t/acre and 25 cm application depth.

Transient conditions are also important to for managing carbon cycling in drylands. In 5 h laboratory experiments, the peak after wetting composed almost 80% of the total CO_2 efflux (Sánchez-García et al., 2020). Transient conditions due to drying and rewetting—even when short-lived—were found to result in higher soil CO_2 emissions than constantly moist soils and gain relevance because of the spatial extent of drylands (Jarvis et al., 2007; Shen et al., 2009).

Shown as comparison to the simulated soil CO_2 efflux is the range of carbonate alkalinity fluxes in rivers in carbonate-dominated catchments (Zhang S. et al., 2022) (Figure 9). Carbonate alkalinity export to rivers derived from calcite correlates with hydrological conditions and carbonate precipitation under dry conditions leads to increased CO_2 soil efflux (Wen et al., 2022). Therein lies a potential benefit of increased gas sorption within carbonate containing soils. Sorption is reversible and desorption of CO_2 that occurs when water is present could aid export of carbonate alkalinity to rivers. How much of the desorbed CO_2 escapes to the atmosphere or is trapped in pore space depends on a myriad of environmental factors, such as water amount and soil properties (Sánchez-García et al., 2020).

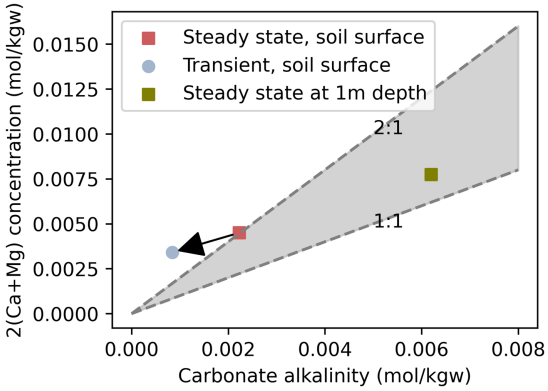

FIGURE 8
Carbonate alkalinity and Ca^{2+} and Mg^{2+} concentrations shown for steady state conditions at the soil-atmosphere interface (red square), transient conditions at the soil-atmosphere interface (blue dot), and steady state conditions at 1 m depth. The lower line depicts the 1:1 ratio expected for carbonate dissolution exclusively from carbonic acid. The upper line depicts 2:1 stoichiometry of calcite dissolution through other acids, e.g., in fertilizer impacted sites. The area above the 2:1 line represents conversion of bicarbonate to CO_2 through degassing.

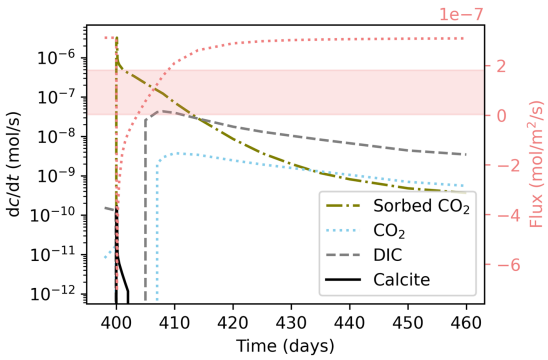

FIGURE 9
Total concentration changes in sorbed CO_2, soil CO_2, DIC in porewater, and calcite over simulation time in comparison with CO_2 efflux from soil (right y-axis). The red area indicates the range of carbonate alkalinity flux in rivers in carbonate-dominated catchments (mol m^{-2} s^{-1}) (data from Zhang S. et al., 2022).

4.2 Implications for application of soil amendments and monitoring of CDR

The simulated dynamics indicate both potential co-benefits and disadvantages for co-application of various soil amendments. Application of soil amendments that cause positive priming might be suitable to be combined with EW, because the increased production of CO_2 could drive mineral dissolution. However, soil amendments that induce negative priming associated with reduced CO_2 production could hinder EW. Biochar can cause positive or negative priming, but the underlying drivers are still poorly understood (El-Naggar et al., 2019). Thus, sites-specific evaluation of the response to biochar may be required.

The simulations have further implications for monitoring established or promising soil CDR methods. CDR via biochar currently only considers C that is contained in biochar, but biochar also affects native soil C. This is why recommendations for monitoring would be relevant for biochar if native soil C is regulated in the future. This is especially important because fragile drylands soils are more vulnerable to climate change (Lal, 2019). Key drivers for carbon cycling, such as temperature and precipitation, are currently changing at a regional scale, while the local response of SOC and SIC pools in drylands is uncertain (Shen et al., 2009; Wang et al., 2022). Depending on specific climatic and soil conditions in drylands, monitoring campaigns need to adequately capture transient conditions over different time scales. If degassing, (de)sorption, and soil gas displacement are expected to play a major role and should be investigated (Sánchez-García et al., 2020), monitoring needs to capture transient conditions that might last only a few hours or days. On the other hand, climates dominated by seasonal variations need to capture these variations over longer time scales and to avoid under-or overestimation of carbon fluxes.

Various monitoring methods need to be applied to distinguish different processes within the carbon cycle. There are a range of parameters that can help to monitor CDR by distinguishing between organic and inorganic carbon cycling. Carbon mass balance over depths, pCO_2 depth profiles, O_2 concentrations or depth profiles, and carbon isotope composition can help to distinguish biotic and abiotic process (Angert et al., 2015; Gallagher and Breecker, 2020). Monitoring major cations and anions is helpful to resolve if carbonate and silicate weathering consumes CO_2 or is driven by other acids (Perrin et al., 2008; Zamanian et al., 2018).

Simulated carbon dynamics are specifically relevant for monitoring of EW. Monitoring of all parameters that are affected by CDR methods like EW can be expensive, which is why monitoring schemes that provide reliable CDR estimates based on as little monitoring as possible are under development and there is no consensus yet on what constitutes a reliable method. Fuhr et al. (2023) also points out that highly dynamic natural background conditions need to be accounted to monitor EW fluxes reliably. Various methods to monitor or predict EW have been presented in the literature: (1) carbonate alkalinity and cation concentrations either in rivers (Knapp and Tipper, 2022; Zhang S. et al., 2022) or in soils (Holzer et al., 2023), (2) Ca, Mg and nitrate ions and rare earth elements (Kantola et al., 2023) (3) total alkalinity (Fuhr et al., 2023), (4) electrical conductivity (Rieder et al., 2023), and (5) simulations of varying complexity and spatial scale (Beerling et al., 2020; Cipolla et al., 2021; Kanzaki et al., 2023). An important process that was highlighted by simulations here and should be considered when monitoring EW is degassing, which resulted in additional removal of DIC from solution as well as short-lived calcite precipitation. Most streams are oversaturated with respect to CO_2 and degassing is prevalent (Stets et al., 2017). Estimates suggest up to 60% of CO_2 emissions from streams originate from DIC (Duvert et al., 2019; Winnick and Saccardi, 2024), and 30% of CO_2 originate from DOC (Khadka et al., 2014). Spatial and temporal patterns of pCO_2, degassing and sources of degassing depend on flow regimes, respiration, alkalinity, and groundwater inputs (Khadka et al., 2014; Winnick and Saccardi, 2024). A positive correlation between the pool of DIC and the contribution of DIC to degassing fluxes has been found (Winnick and Saccardi, 2024). In the simulations, degassing and removal of DIC also led to calcite precipitation. However many rivers are supersaturated with respect to calcite potentially due to inhibition (Knapp and Tipper, 2022).

4.3 Carbon sequestration potential

The simulations show that abiotic C-sinks such as CO_2 sorption gain importance as a C sink in soils when biological activity is low, which is the case in many dryland ecosystems (Warner et al., 2019; Sagi et al., 2021). The relative reduction in CO_2 efflux over relaxation time was higher with lower CO_2 production (Figure 5). Moreover, dryland soils with low organic matter content have the lowest sorption capacity of all naturally occurring soils and around 10 times lower sorption capacity than the simulated sorbents (De Jonge and Mittelmeijer-Hazeleger, 1996; Ravikovitch et al., 2005; Davidson et al., 2013). Although CDR through sorption is estimated to be relatively low for a single application (around 2% of total C for the simulated biochar as detailed in SI), soil amendments could be relevant for drylands due to the limitations of other methods and through provision of soil health benefits.

4.4 Additional considerations for soil amendments in drylands

Soil amendments have the co-benefit of alleviating soil degradation, specifically salinization. Soil salinity is a worldwide concern, with drylands, irrigated lands, and agricultural lands most at risk (Dregne et al., 1991; Ivushkin et al., 2019). Mechanisms that have been implicated in salinity amelioration with biochar are: release of Ca^{2+} and Mg^{2+}, adsorption of Na^+, proton release that promotes Na^+ uptake in certain plant species, increased salt leaching through increased porosity (Akhtar et al., 2015; Amini et al., 2016), reduced EC (Lashari et al., 2015), and changes in evaporation dynamics (Liang et al., 2021; Lee et al., 2022). However, depending on biochar characteristics biochar could release Na^+ (Saifullah Dahlawi et al., 2018) and some biochar studies have been criticized because salt stress was induced with NaCl (Akhtar et al., 2015).

Challenges for soil amendment application are health risks, transport emission and albedo changes. Although biochar feedstock can contain heavy metals and organic contaminants, the fraction that is bioavailable after pyrolysis tends to be small (Godlewska et al., 2021). Sorbent materials generally immobilize contaminants if the sorbent is immobile (Godlewska et al., 2021) suggesting positive health effects. Soil amendments can lead to reduced wind erosion long-term, which could be an important benefit for drylands (Şeker and Manirakiza, 2020; Pi et al., 2021).

Emissions from implementation, e.g., material preparation and transport will reduce the CDR potential. Transport emissions are a particular concern, because there is typically little infrastructure in drylands. Sources for biochar are scarce in drylands due to relatively lower above ground biomass (Cook-Patton et al., 2020), however, most of the global irrigated lands are situated on drylands (Dregne et al., 1991; Siebert et al., 2015) and could provide biomass sources, as could other organic wastes.

Albedo refers to surface albedo, which varies by land cover type, color, wetness and surface irregularities (Zhang X. et al., 2022). Albedo is highest in deserts (0.2–0.45) and dry soils (0.15–0.36) while increased water content (0.06–0.19) and vegetation cover reduce albedo (grasses 0.2, savannah 0.15–0.2) (Garratt, 1993). Biochar application was found to lead to albedo reduction of 0.05 on agricultural soil, which lowered the predicted climate change mitigation benefit by 13–22% (Meyer et al., 2012). The changes in soil albedo are less of a concern for vegetated grasslands and shrublands, which make up around two thirds of global drylands. Future work should assess albedo changes in field trials.

5 Summary

Reactive transport simulations were performed to investigate dynamics between organic and inorganic C pools in dryland soils and to predict CDR via CO_2 sorption on soil amendments. In the simulations, CDR via sorption gained importance when biological activity was low – transient conditions lasted longer and a larger percentage of CO_2 was prevented from efflux during those transient conditions. Simulations highlighted that CO_2 removal via sorption causes transient conditions affecting CO_2 efflux, pCO_2, DIC, pH, major cations and calcite. The simulated dynamics have implications for the application of a range of CDR methods, e.g., if the combined application of biochar and minerals for enhanced rock weathering will benefit CDR depends on soil priming effects. The transient conditions have implications for monitoring: the presence of carbonates, degassing, and desorption can affect the timing and magnitude of the soil CO_2 response, which needs to be considered in sampling schedules or sampling parameters. Future work should include evaluation of different sorbent designs, transport modes, and albedo changes. Considering that a high percentage of dryland soils are degraded and that other methods are limited by water availability, soil amendments with high sorption potential and soil health benefits could provide valuable CDR potential and aid restoration of dryland soils.

Data availability statement

The original contributions presented in the study are included in the article/Supplementary material, further inquiries can be directed to the corresponding author.

Author contributions

SH: Conceptualization, Formal analysis, Methodology, Visualization, Writing – original draft, Writing – review & editing. AJR: Data curation, Writing – review & editing. KM: Conceptualization, Funding acquisition, Methodology, Supervision, Writing – review & editing.

Funding

The author(s) declare that financial support was received for the research, authorship, and/or publication of this article. The authors gratefully acknowledge support from the Stanford Doerr School of Sustainability Accelerator Program. AJR acknowledges support from the National Science Foundation Graduate Research Fellowship Program under Award DGE-1656518.

Conflict of interest

The authors declare that the research was conducted in the absence of any commercial or financial relationships that could be construed as a potential conflict of interest.

Generative AI statement

The authors declare that no Generative AI was used in the creation of this manuscript.

Publisher's note

All claims expressed in this article are solely those of the authors and do not necessarily represent those of their affiliated organizations, or those of the publisher, the editors and the reviewers. Any product that may be evaluated in this article, or claim that may be made by its manufacturer, is not guaranteed or endorsed by the publisher.

Supplementary material

The Supplementary material for this article can be found online at: https://www.frontiersin.org/articles/10.3389/fclim.2025.1505472/full#supplementary-material

References

Akhtar, S. S., Andersen, M. N., and Liu, F. (2015). Residual effects of biochar on improving growth, physiology and yield of wheat under salt stress. *Agric. Water Manag.* 158, 61–68. doi: 10.1016/j.agwat.2015.04.010

Al Mesfer, M. K., Danish, M., Khan, M. I., Ali, I. H., Hasan, M., and Jery, A. (2020). Continuous fixed bed CO_2 adsorption: breakthrough, column efficiency, mass transfer zone. *PRO* 8, 1–16. doi: 10.3390/pr8101233

Amini, S., Ghadiri, H., Chen, C., and Marschner, P. (2016). Salt-affected soils, reclamation, carbon dynamics, and biochar: a review. *J. Soils Sediments* 16, 939–953. doi: 10.1007/s11368-015-1293-1

Amundson, R., Stern, L., Baisden, T., and Wang, Y. (1998). The isotopic composition of soil and soil-respired CO_2. *Geoderma* 82, 83–114. doi: 10.1016/S0016-7061(97)00098-0

Angert, A., Yakir, D., Rodeghiero, M., Preisler, Y., Davidson, E. A., and Weiner, T. (2015). Using O_2 to study the relationships between soil CO_2 efflux and soil respiration. *Biogeosciences* 12, 2089–2099. doi: 10.5194/bg-12-2089-2015

Beerling, D. J., Kantzas, E. P., Lomas, M. R., Wade, P., Eufrasio, R. M., Renforth, P., et al. (2020). Potential for large-scale CO_2 removal via enhanced rock weathering with croplands. *Nature* 583, 242–248. doi: 10.1038/s41586-020-2448-9

Berg, A., and McColl, K. A. (2021). No projected global drylands expansion under greenhouse warming. *Nat. Clim. Chang.* 11, 331–337. doi: 10.1038/s41558-021-01007-8

Breecker, D. O., Sharp, Z. D., and McFadden, L. D. (2009). Seasonal bias in the formation and stable isotopic composition of pedogenic carbonate in modern soils from Central New Mexico, USA. *GSA Bull.* 121, 630–640. doi: 10.1130/B26413.1

Calabrese, S., Wild, B., Bertagni, M. B., Bourg, I. C., White, C., Aburto, F., et al. (2022). Nano- to global-scale uncertainties in terrestrial enhanced weathering. *Environ. Sci. Technol.* 56, 15261–15272. doi: 10.1021/acs.est.2c03163

Cerling, T. E. (1984). The stable isotopic composition of modern soil carbonate and its relationship to climate. *Earth Planet. Sci. Lett.* 71, 229–240. doi: 10.1016/0012-821X(84)90089-X

Chadwick, O. A., Derry, L. A., Vitousek, P. M., Huebert, B. J., and Hedin, L. O. (1999). Changing sources of nutrients during four million years of ecosystem development. *Nature* 397, 491–497. doi: 10.1038/17276

Chausson, A., Turner, B., Seddon, D., Chabaneix, N., Girardin, C. A. J., Kapos, V., et al. (2020). Mapping the effectiveness of nature-based solutions for climate change adaptation. *Glob. Chang. Biol.* 26, 6134–6155. doi: 10.1111/gcb.15310

Cherlet, M., Hutchinson, C., Reynolds, J., Hill, J., Sommer, S., and Von Maltitz, G. (Eds.) (2018). World atlas of desertification. Luxembourg: Publication Office of the European Union.

Chirinda, N., Plauborg, F., Heckrath, G., Elsgaard, L., Thomsen, I. K., and Olesen, J. E. (2014). Carbon dioxide in arable soil profiles: a comparison of automated and manual measuring systems. *Commun. Soil Sci. Plant Anal.* 45, 1278–1291. doi: 10.1080/00103624.2014.884107

Cipolla, G., Calabrese, S., Noto, L. V., and Porporato, A. (2021). The role of hydrology on enhanced weathering for carbon sequestration I. Modeling rock-dissolution reactions coupled to plant, soil moisture, and carbon dynamics. *Adv. Water Resour.* 154:103934. doi: 10.1016/j.advwatres.2021.103934

Cook-Patton, S. C., Leavitt, S. M., Gibbs, D., Harris, N. L., Lister, K., Anderson-teixeira, K. J., et al. (2020). Mapping carbon accumulation potential from global natural forest regrowth. *Nature* 585, 545–550. doi: 10.1038/s41586-020-2686-x

Currie, J. A. (1960). Gaseous diffusion in porous media part 1. - a non-steady state method. *Br. J. Appl. Phys.* 11, 314–317. doi: 10.1088/0508-3443/11/8/302

Darrouzet-Nardi, A., Reed, S. C., Grote, E. E., and Belnap, J. (2015). Observations of net soil exchange of CO2 in a dryland show experimental warming increases carbon losses in biocrust soils. *Biogeochemistry* 126, 363–378. doi: 10.1007/s10533-015-0163-7

Davidson, G. R., Phillips-housley, A., and Stevens, M. T. (2013). Soil-zone adsorption of atmospheric CO_2 as a terrestrial carbon sink. *Geochim. Cosmochim. Acta* 106, 44–50. doi: 10.1016/j.gca.2012.12.015

Davidson, E. A., Savage, K. E., Trumbore, S. E., and Borken, W. (2006). Vertical partitioning of CO2 production within a temperate forest soil. *Glob. Chang. Biol.* 12, 944–956. doi: 10.1111/j.1365-2486.2005.01142.x

De Jonge, H., and Mittelmeijer-Hazeleger, M. C. (1996). Adsorption of CO_2 and N_2 on soil organic matter: nature of porosity, surface area, and diffusion mechanisms. *Environ. Sci. Technol.* 30, 408–413. doi: 10.1021/es950043t

Domínguez-villar, D., Bensa, A., Svob, M., Krklec, K., and Rossa, T. (2022). Causes and implications of the seasonal dissolution and precipitation of pedogenic carbonates in soils of karst regions – a thermodynamic model approach. *Geoderma* 423:115962. doi: 10.1016/j.geoderma.2022.115962

Dong, X., Singh, B. P., Li, G., Lin, Q., and Zhao, X. (2019). Biochar increased field soil inorganic carbon content five years after application. *Soil Tillage Res.* 186, 36–41. doi: 10.1016/j.still.2018.09.013

Doni, S., Gispert, M., Peruzzi, E., Macci, C., Mattii, G. B., Manzi, D., et al. (2021). Impact of natural zeolite on chemical and biochemical properties of vineyard soils. *Soil Use Manag.* 37, 832–842. doi: 10.1111/sum.12665

Dou, Y., Howard, K. W. F., and Qian, H. (2016). Transport characteristics of nitrite in a shallow sedimentary aquifer in Northwest China as determined by a 12-day soil column experiment. *Expo. Heal.* 8, 381–387. doi: 10.1007/s12403-016-0206-x

Dregne, H. E., Kassas, M., and Rozanov, B. (1991). A new assessment of the world status of desertification. *Desertification Control Bullet.* 20, 7–18.

Duvert, C., Bossa, M., Tyler, K. J., Wynn, J. G., Munksgaard, N. C., Bird, M. I., et al. (2019). Groundwater-derived DIC and carbonate buffering enhance fluvial CO2 evasion in two Australian tropical rivers. *J. Geophys. Res. Biogeosciences* 124, 312–327. doi: 10.1029/2018JG004912

El-Naggar, A., El-Naggar, A. H., Shaheen, S. M., Sarkar, B., Chang, S. X., Tsang, D. C. W., et al. (2019). Biochar composition-dependent impacts on soil nutrient release, carbon mineralization, and potential environmental risk: a review. *J. Environ. Manag.* 241, 458–467. doi: 10.1016/j.jenvman.2019.02.044

Fan, R., Zhang, B., Li, J., Zhang, Z., and Liang, A. (2020). Straw-derived biochar mitigates CO2 emission through changes in soil pore structure in a wheat-rice rotation system. *Chemosphere* 243:125329. doi: 10.1016/j.chemosphere.2019.125329

Ferguson, P. R., and Veizer, J. (2007). Coupling of water and carbon fluxes via the terrestrial biosphere and its significance to the Earth's climate system. *J. Geophys. Res. Atmos.* 112, 1–17. doi: 10.1029/2007JD008431

Figini-Albisetti, A., Velasco, L. F., Parra, J. B., and Ania, C. O. (2010). Effect of outgassing temperature on the performance of porous materials. *Appl. Surf. Sci.* 256, 5182–5186. doi: 10.1016/j.apsusc.2009.12.090

Francis, J. C., Nighojkar, A., and Kandasubramanian, B. (2023). Relevance of wood biochar on CO_2 adsorption: a review. *Hybrid Adv.* 3:100056. doi: 10.1016/j.hybadv.2023.100056

Freeze, R., and Cherry, J. (1979). Groundwater contamination. Hoboken, NJ: Prentice Hall.

Fuhr, M., Wallmann, K., Dale, A. W., Diercks, I., Kalapurakkal, H. T., Schmidt, M., et al. (2023). Disentangling artificial and natural benthic weathering in organic rich Baltic Sea sediments. *Front. Clim.* 5:1245580. doi: 10.3389/fclim.2023.1245580

Gaillardet, J., Dupre, B., Louvat, P., and Allegre, C. J. (1999). Global silicate weathering and CO2 consumption rates deduced from the chemistry of large rivers. *Chem. Geol.* 159, 3–30. doi: 10.1016/S0009-2541(99)00031-5

Gallagher, T. M., and Breecker, D. O. (2020). The obscuring effects of calcite dissolution and formation on quantifying soil respiration. *Global Biogeochem. Cycles* 34:e2020GB006584. doi: 10.1029/2020GB006584

Garbowski, T., Bar-Michalczyk, D., Charazińska, S., Grabowska-Polanowska, B., Kowalczyk, A., and Lochyński, P. (2023). An overview of natural soil amendments in agriculture. *Soil Tillage Res.* 225:105462. doi: 10.1016/j.still.2022.105462

Garratt, J. R. (1993). Sensitivity of climate simulations to land-surface and atmospheric boundary-layer treatments - a review. *J. Clim.* 6, 419–448. doi: 10.1175/1520-0442(1993)006<0419:SOCSTL>2.0.CO;2

Godlewska, P., Ok, Y. S., and Oleszczuk, P. (2021). The dark side of black gold: Ecotoxicological aspects of biochar and biochar-amended soils. *J. Hazard. Mater.* 403:123833. doi: 10.1016/j.jhazmat.2020.123833

Gray, M., Johnson, M. G., Dragila, M. I., and Kleber, M. (2014). Water uptake in biochars: the roles of porosity and hydrophobicity. *Biomass Bioenergy* 61, 196–205. doi: 10.1016/j.biombioe.2013.12.010

Griscom, B. W., Adams, J., Ellis, P. W., Houghton, R. A., Lomax, G., Miteva, D. A., et al. (2017). Natural climate solutions. *PNAS Nexus* 114, 11645–11650. doi: 10.1073/pnas.1710465114

Halliday, C., and Hatton, T. A. (2021). Sorbents for the capture of CO_2 and other acid gases: a review. *Ind. Eng. Chem. Res.* 60, 9313–9346. doi: 10.1021/acs.iecr.1c00597

Holzer, I. O., Nocco, M. A., and Houlton, B. Z. (2023). Direct evidence for atmospheric carbon dioxide removal via enhanced weathering in cropland soil. *Environ. Res. Commun.* 5:acfd89. doi: 10.1088/2515-7620/acfd89

Ivushkin, K., Bartholomeus, H., Bregt, A. K., Pulatov, A., Kempen, B., and de Sousa, L. (2019). Global mapping of soil salinity change. *Remote Sens. Environ.* 231:111260. doi: 10.1016/j.rse.2019.111260

Jarosz, R., Szerement, J., Gondek, K., and Mierzwa-hersztek, M. (2022). The use of zeolites as an addition to fertilisers – a review. *Catena* 213:106125. doi: 10.1016/j.catena.2022.106125

Jarvis, P., Rey, A., Petsikos, C., Wingate, L., Pereira, J., Banza, J., et al. (2007). Drying and wetting of Mediterranean soils stimulates decomposition and carbon dioxide emission: the "birch effect. *Tree Physiol.* 27, 929–940. doi: 10.1093/treephys/27.7.929

Jia, M., Jacques, D., Gérard, F., Su, D., Mayer, K. U., and Šimůnek, J. (2021). A benchmark for soil organic matter degradation under variably saturated flow conditions. *Comput. Geosci.* 25, 1359–1377. doi: 10.1007/s10596-019-09862-3

Kantola, I. B., Blanc-Betes, E., Masters, M. D., Chang, E., Marklein, A., Moore, C. E., et al. (2023). Improved net carbon budgets in the US Midwest through direct measured impacts of enhanced weathering. *Glob. Chang. Biol.* 29, 7012–7028. doi: 10.1111/gcb.16903

Kanzaki, Y., Planavsky, N. J., and Reinhard, C. T. (2023). New estimates of the storage permanence and ocean co-benefits of enhanced rock weathering. *PNAS Nexus* 2, 1–9. doi: 10.1093/pnasnexus/pgad059

Kaur, B., Gupta, R. K., and Bhunia, H. (2019). Chemically activated nanoporous carbon adsorbents from waste plastic for CO_2 capture: breakthrough adsorption study. *Microporous Mesoporous Mater.* 282, 146–158. doi: 10.1016/j.micromeso.2019.03.025

Kemper, W. D., Rosenau, R., and Nelson, S. (1985). Gas displacement and aggregate stability of soils. *Soil Sci. Soc. Am. J.* 49, 25–28. doi: 10.2136/sssaj1985.03615995004900010004x

Khadka, M. B., Martin, J. B., and Jin, J. (2014). Transport of dissolved carbon and CO_2 degassing from a river system in a mixed silicate and carbonate catchment. *J. Hydrol.* 513, 391–402. doi: 10.1016/j.jhydrol.2014.03.070

Knapp, W. J., and Tipper, E. T. (2022). The efficacy of enhancing carbonate weathering for carbon dioxide sequestration. *Front. Clim.* 4:928215. doi: 10.3389/fclim.2022.928215

Kwon, S., and Pignatello, J. J. (2005). Effect of natural organic substances on the surface and adsorptive properties of environmental black carbon (char): Pseudo pore blockage by model lipid components and its implications for N2-probed surface properties of natural sorbents. *Environ. Sci. Technol.* 39, 7932–7939. doi: 10.1021/es050976h

Lal, R., Kimble, J. M., Stewart, B. A., and Eswaran, H. (2000). Global climate change and pedogenic carbonates. Lewis Publishers.

Lal, R. (2004). Carbon sequestration in dryland ecosystems. *Environ. Manag.* 33, 528–544. doi: 10.1007/s00267-003-9110-9

Lal, R. (2019). Carbon cycling in global drylands. *Curr. Clim. Chang. Reports* 5, 221–232. doi: 10.1007/s40641-019-00132-z

Lal, R. (2020). Managing soils for negative feedback to climate change and positive impact on food and nutritional security. *Soil Sci. Plant Nutr.* 66, 1–9. doi: 10.1080/00380768.2020.1718548

Lal, R., Monger, C., Nave, L., and Smith, P. (2021). The role of soil in regulation of climate. *Philos. Trans. R. Soc. B* 376:20210084. doi: 10.1098/rstb.2021.0084

Lashari, M. S., Ye, Y., Ji, H., Li, L., Kibue, G. W., Lu, H., et al. (2015). Biochar-manure compost in conjunction with pyroligneous solution alleviated salt stress and improved leaf bioactivity of maize in a saline soil from Central China: a 2-year field experiment. *J. Sci. Food Agric.* 95, 1321–1327. doi: 10.1002/jsfa.6825

Lee, X., Yang, F., Xing, Y., Huang, Y., Xu, L., Liu, Z., et al. (2022). Use of biochar to manage soil salts and water: effects and mechanisms. *Catena* 211:106018. doi: 10.1016/j.catena.2022.106018

Lehmann, J., Cowie, A., Masiello, C. A., Kammann, C., Woolf, D., Amonette, J. E., et al. (2021). Biochar in climate change mitigation. *Nat. Geosci.* 14, 883–892. doi: 10.1038/s41561-021-00852-8

Lehmann, N., Lantuit, H., Böttcher, M. E., Hartmann, J., Eulenburg, A., and Thomas, H. (2023). Alkalinity generation from carbonate weathering in a silicate-dominated headwater catchment at Iskorasfjellet, northern Norway. *Biogeosciences* 20, 3459–3479. doi: 10.5194/bg-20-3459-2023

Lehmann, J., and Rondon, M. (2006). Bio-char soil management on highly weathered soils in the humid tropics. *Biol. Approaches Sust. Soil Syst.* 22, 517–529. doi: 10.1201/9781420017113.ch36

Liang, J., Li, Y., Si, B., Wang, Y., Chen, X., Wang, X., et al. (2021). Optimizing biochar application to improve soil physical and hydraulic properties in saline-alkali soils. *Sci. Total Environ.* 771:144802. doi: 10.1016/j.scitotenv.2020.144802

Limousin, G., Gaudet, J. P., Charlet, L., Szenknect, S., Barthès, V., and Krimissa, M. (2007). Sorption isotherms: a review on physical bases, modeling and measurement. *Appl. Geochem.* 22, 249–275. doi: 10.1016/j.apgeochem.2006.09.010

Liu, S., Zhang, Y., Zong, Y., Hu, Z., Wu, S., Zhou, J., et al. (2016). Response of soil carbon dioxide fluxes, soil organic carbon and microbial biomass carbon to biochar amendment: a meta-analysis. *GCB Bioenergy* 8, 392–406. doi: 10.1111/gcbb.12265

Lu, T., Wang, X., Du, Z., and Wu, L. (2021). Impacts of continuous biochar application on major carbon fractions in soil profile of North China Plain's cropland: in comparison with straw incorporation. *Agric. Ecosyst. Environ.* 315:107445. doi: 10.1016/j.agee.2021.107445

Meyer, S., Bright, R. M., Fischer, D., Schulz, H., and Glaser, B. (2012). Albedo impact on the suitability of biochar systems to mitigate global warming. *Environ. Sci. Technol.* 46, 12726–12734. doi: 10.1021/es302302g

Millington, R. J. (1958). Gas diffusion in porous media. *Science* 130, 100–102. doi: 10.1126/science.130.3367.100.b

Mondal, M., Biswas, B., Garai, S., Sarkar, S., Banerjee, H., Brahmachari, K., et al. (2021). Zeolites enhance soil health, crop productivity and environmental safety. *Agronomy* 11:448. doi: 10.3390/agronomy11030448

Monger, H. C., and Gallegos, R. A. (2000). Biotic and abiotic processes and rates of pedogenic carbonate accumulation in the southwestern United States-relationship to atmoshperic CO_2 sequestration. *Global Clim. Change Pedogenic Carbon.* 22, 273–290.

Monger, H. C., Kraimer, R. A., Khresat, S., Cole, D. R., Wang, X., and Wang, J. (2015). Sequestration of inorganic carbon in soil and groundwater. *Geology* 43, 375–378. doi: 10.1130/G36449.1

Mosa, A., Mansour, M. M., Soliman, E., El-Ghamry, A., El Alfy, M., and El Kenawy, A. M. (2023). Biochar as a soil amendment for restraining greenhouse gases emission and improving soil carbon sink: current situation and ways forward. *Sustain. For.* 15:206. doi: 10.3390/su15021206

Naorem, A., Jayaraman, S., Dalal, R. C., Patra, A., Rao, C. S., and Lal, R. (2022). Soil inorganic carbon as a potential sink in carbon storage in dryland soils—a review. *Agriculture* 12, 1–20. doi: 10.3390/agriculture12081256

Nepal, J., Ahmad, W., Munsif, F., Khan, A., and Zou, Z. (2023). Advances and prospects of biochar in improving soil fertility, biochemical quality, and environmental applications. *Front. Environ. Sci.* 11:1114752. doi: 10.3389/fenvs.2023.1114752

Oertel, C., Matschullat, J., Zurba, K., Zimmermann, F., and Erasmi, S. (2016). Greenhouse gas emissions from soils—a review. *Chem. Erde* 76, 327–352. doi: 10.1016/j.chemer.2016.04.002

Pal, A., Chand, S., Madden, D. G., Franz, D., Ritter, L., Johnson, A., et al. (2019). A microporous co-MOF for highly selective CO_2 sorption in high loadings involving aryl C-H···O=C=O interactions: combined simulation and breakthrough studies. *Inorg. Chem.* 58, 11553–11560. doi: 10.1021/acs.inorgchem.9b01402

Perrin, A. S., Probst, A., and Probst, J. L. (2008). Impact of nitrogenous fertilizers on carbonate dissolution in small agricultural catchments: implications for weathering CO2 uptake at regional and global scales. *Geochim. Cosmochim. Acta* 72, 3105–3123. doi: 10.1016/j.gca.2008.04.011

Pfeiffer, M., Padarian, J., and Vega, M. P. (2023). Soil inorganic carbon distribution, stocks and environmental thresholds along a major climatic gradient. *Geoderma* 433:116449. doi: 10.1016/j.geoderma.2023.116449

Pi, H., Huggins, D. R., and Sharratt, B. (2021). Wind erosion of soil influenced by clay amendment in the inland Pacific northwest, USA. *L. Degrad. Dev* 32, 241–255. doi: 10.1002/ldr.3709

Prăvălie, R. (2016). Drylands extent and environmental issues. A global approach. *Earth-Sci. Rev.* 161, 259–278. doi: 10.1016/j.earscirev.2016.08.003

Priddle, M. W., and Jackson, R. E. (1991). Laboratory column measurement of VOC retardation factors and comparison with field values. *Groundwater* 29, 260–266. doi: 10.1111/j.1745-6584.1991.tb00518.x

Prince, S. D. (2016). "Where does desertification occur? Mapping dryland degradation at regional to global scales" in The end of desertification? eds. R. Behnke and M. Mortimore (Berlin: Springer Berlin Heidelberg), 225–263.

Ravikovitch, P. I., Bogan, B. W., and Neimark, A. V. (2005). Nitrogen and carbon dioxide adsorption by soils. *Environ. Sci. Technol.* 39, 4990–4995. doi: 10.1021/es048307b

Reynolds, J. F., Smith, D. M. S., Lambin, E. F., Ii, B. L. T., Mortimore, M., Batterbury, S. P. J., et al. (2007). Global desertification: building a science for dryland development. *Science* 316, 847–851. doi: 10.1126/science.1131634

Rieder, L., Amann, T., and Hartmann, J. (2023). Soil electrical conductivity as a proxy for enhanced weathering in soils. *Front. Clim.* 5:1283107. doi: 10.3389/fclim.2023.1283107

Ringsby, A. J., Ross, C. M., and Maher, K. (2024). Sorption of soil carbon dioxide by biochar and engineered porous carbons. *Environ. Sci. Technol.* 58, 8313–8325. doi: 10.1021/acs.est.4c02015

Roe, S., Streck, C., Beach, R., Busch, J., Chapman, M., Daioglou, V., et al. (2021). Land-based measures to mitigate climate change: potential and feasibility by country. *Glob. Chang. Biol.* 27, 6025–6058. doi: 10.1111/gcb.15873

Rolston, D. E., and Moldrup, P. (2002). Gas diffusivity. *Methods Soil Anal.* 5, 1113–1139. doi: 10.2136/sssabookser5.4.c45

Sagi, N., Zaguri, M., and Hawlena, D. (2021). Soil CO_2 influx in drylands: a conceptual framework and empirical examination. *Soil Biol. Biochem.* 156:108209. doi: 10.1016/j.soilbio.2021.108209

Saifullah Dahlawi, S., Naeem, A., Rengel, Z., and Naidu, R. (2018). Biochar application for the remediation of salt-affected soils: challenges and opportunities. *Sci. Total Environ.* 625, 320–335. doi: 10.1016/j.scitotenv.2017.12.257

Sánchez-García, C., Doerr, S. H., and Urbanek, E. (2020). The effect of water repellency on the short-term release of CO_2 upon soil wetting. *Geoderma* 375:114481. doi: 10.1016/j.geoderma.2020.114481

Sanderman, J., Hengl, T., and Fiske, G. J. (2017). Soil carbon debt of 12,000 years of human land use. *Proc. Natl. Acad. Sci. U. S. A.* 114, 9575–9580. doi: 10.1073/pnas.1706103114

Schlesinger, W. H. (2017). An evaluation of abiotic carbon sinks in deserts. *Glob. Chang. Biol.* 23, 25–27. doi: 10.1111/gcb.13336

Seddon, N., Chausson, A., Berry, P., Girardin, C. A. J., Smith, A., Turner, B., et al. (2020). Understanding the value and limits of nature-based solutions to climate change and other global challenges. *Philos. Trans. Royel Soc. B* 375:20190120. doi: 10.1098/rstb.2019.0120

Şeker, C., and Manirakiza, N. (2020). Effectiveness of compost and biochar in improving water retention characteristics and aggregation of sandy clay loam soil under wind erosion. *Carpathian J. Earth Environ. Sci.* 15, 5–18. doi: 10.26471/cjees/2020/015/103

Semhi, K., Amiotte Suchet, P., Clauer, N., and Probst, J. L. (2000). Impact of nitrogen fertilizers on the natural weathering-erosion processes and fluvial transport in the Garonne basin. *Appl. Geochem.* 15, 865–878. doi: 10.1016/S0883-2927(99)00076-1

Sha, Y., Chi, D., Chen, T., Wang, S., Zhao, Q., Li, Y., et al. (2022). Zeolite application increases grain yield and mitigates greenhouse gas emissions under alternate wetting and drying rice system. *Sci. Total Environ.* 838:156067. doi: 10.1016/j.scitotenv.2022.156067

Shen, W., Reynolds, J. F., and Hui, D. (2009). Responses of dryland soil respiration and soil carbon pool size to abrupt vs. gradual and individual vs. combined changes in soil temperature, precipitation, and atmospheric [CO_2]: a simulation analysis. *Glob. Chang. Biol.* 15, 2274–2294. doi: 10.1111/j.1365-2486.2009.01857.x

Siebert, S., Kummu, M., Porkka, M., Döll, P., Ramankutty, N., and Scanlon, B. R. (2015). A global data set of the extent of irrigated land from 1900 to 2005. *Hydrol. Earth Syst. Sci.* 19, 1521–1545. doi: 10.5194/hess-19-1521-2015

Spokas, K. A., Novak, J. M., Masiello, C. A., Johnson, M. G., Colosky, E. C., Ippolito, J. A., et al. (2014). Physical disintegration of biochar: an overlooked process. *Environ. Sci. Technol. Lett.* 1, 326–332. doi: 10.1021/ez500199t

Steefel, C. I., Appelo, C. A. J., Arora, B., Jacques, D., Kalbacher, T., Kolditz, O., et al. (2015). Reactive transport codes for subsurface environmental simulation. *Comput. Geosci.* 19, 445–478. doi: 10.1007/s10596-014-9443-x

Stets, E. G., Butman, D., McDonald, C. P., Stackpoole, S. M., DeGrandpre, M. D., and Striegl, R. G. (2017). Carbonate buffering and metabolic controls on carbon dioxide in rivers. *Global Biogeochem. Cycles* 31, 663–677. doi: 10.1002/2016GB005578

Tang, J., Baldocchi, D. D., Qi, Y., and Xu, L. (2003). Assessing soil CO_2 efflux using continuous measurements of CO_2 profiles in soils with small solid-state sensors. *Agric. For. Meteorol.* 118, 207–220. doi: 10.1016/S0168-1923(03)00112-6

Thengane, S. K., Kung, K., Hunt, J., Gilani, H. R., Lim, C. J., Sokhansanj, S., et al. (2021). Market prospects for biochar production and application in California. *Biofuels Bioprod. Biorefining* 15, 1802–1819. doi: 10.1002/bbb.2280

Unger, S., Máguas, C., Pereira, J. S., David, T. S., and Werner, C. (2010). The influence of precipitation pulses on soil respiration - assessing the "birch effect" by stable carbon isotopes. *Soil Biol. Biochem.* 42, 1800–1810. doi: 10.1016/j.soilbio.2010.06.019

Verstraete, M. M., Hutchinson, C. F., Grainger, A., Stafford Smith, M., Scholes, R. J., Reynolds, J. F., et al. (2011). Towards a global drylands observing system: observational requirements and institutional solutions. *L. Degrad. Dev.* 22, 198–213. doi: 10.1002/ldr.1046

Wang, Y. Y., Hu, C. S., Ming, H., Zhang, Y. M., Li, X. X., Dong, W. X., et al. (2013). Concentration profiles of CH4, CO2 and N2O in soils of a wheat-maize rotation ecosystem in North China plain, measured weekly over a whole year. *Agric. Ecosyst. Environ.* 164, 260–272. doi: 10.1016/j.agee.2012.10.004

Wang, L., Jiao, W., MacBean, N., Rulli, M. C., Manzoni, S., Vico, G., et al. (2022). Dryland productivity under a changing climate. *Nat. Clim. Chang.* 12, 981–994. doi: 10.1038/s41558-022-01499-y

Wang, X., Wang, J., Xu, M., Zhang, W., Fan, T., and Zhang, J. (2015). Carbon accumulation in arid croplands of Northwest China: Pedogenic carbonate exceeding organic carbon. *Sci. Rep.* 5, 1–12. doi: 10.1038/srep11439

Warner, D. L., Bond-Lamberty, B., Jian, J., Stell, E., and Vargas, R. (2019). Spatial predictions and associated uncertainty of annual soil respiration at the global scale global biogeochemical cycles. *Global Biogeochem. Cycles* 33, 1733–1745. doi: 10.1029/2019GB006264

Wen, H., Sullivan, P. L., Billings, S. A., Ajami, H., Cueva, A., Flores, A., et al. (2022). From soils to streams: connecting terrestrial carbon transformation, chemical weathering, and solute export across hydrological regimes. *Water Resour. Res.* 58, 1–26. doi: 10.1029/2022WR032314

Winnick, M. J., Lawrence, C. R., Druhan, J. L., and Maher, K. (2020). Soil respiration response to rainfall modulated by plant phenology in a montane meadow, East River, Colorado, USA. *Adv. Earth Sp. Sci.* 125:5924. doi: 10.1029/2020JG005924

Winnick, M. J., and Saccardi, B. (2024). Impacts of carbonate buffering on atmospheric equilibration of CO_2, δ13CDIC, and Δ14CDIC in rivers and streams. *Global Biogeochem. Cycles* 38:7860. doi: 10.1029/2023GB007860

Wolery, T. J. (1992). EQ3/6, a software package for geochemical modeling of aqueous systems: package overview and installation guide (version 7.0). Livermore, CA: Lawrence Livermore National Lab.

Zamanian, K., Zarebanadkouki, M., and Kuzyakov, Y. (2018). Nitrogen fertilization raises CO_2 efflux from inorganic carbon: a global assessment. *Glob. Chang. Biol.* 24, 2810–2817. doi: 10.1111/gcb.14148

Zeng, S., Liu, Z., and Groves, C. (2022). Large-scale CO_2 removal by enhanced carbonate weathering from changes in land-use practices. *Earth-Sci. Rev.* 225:103915. doi: 10.1016/j.earscirev.2021.103915

Zhang, X., Jiao, Z., Zhao, C., Qu, Y., Liu, Q., and Zhang, H. (2022). Review of land surface albedo: variance characteristics, climate effect and management strategy. *Remote Sens.* 14, 1–28. doi: 10.3390/rs14061382

Zhang, S., Planavsky, N. J., Katchinoff, J., Raymond, P. A., Kanzaki, Y., Reershemius, T., et al. (2022). River chemistry constraints on the carbon capture potential of surficial enhanced rock weathering. *Limnol. Oceanogr.* 67, S148–S157. doi: 10.1002/lno.12244

Zhang, W., Wang, X., Lu, T., Shi, H., and Zhao, Y. (2020). Influences of soil properties and hydrological processes on soil carbon dynamics in the cropland of North China plain. *Agric. Ecosyst. Environ.* 295:106886. doi: 10.1016/j.agee.2020.106886